

# Image amplifier based on Yb<sup>3+</sup>-doped multi-core phosphate optical fiber

S. Suzuki<sup>1,2</sup>, S. Jiang<sup>1</sup>, N. Peyghambarian<sup>1,2</sup>, and A. Chavez-Pirson<sup>1\*</sup>

<sup>1</sup>NP Photonics Inc., 9030 S. Rita Road, Tucson, Arizona 85747

<sup>2</sup>College of Optical Sciences, The University of Arizona, Tucson, Arizona 85721

\*[chavez@npphotonics.com](mailto:chavez@npphotonics.com)

**Abstract:** We demonstrate image amplification with a 19-pixel optical image amplifier array based on high gain per unit length Yb<sup>3+</sup>-doped phosphate glass optical fiber. The 19 pixels of the image amplifier provide spatially uniform image amplification whose gain can reach 30 dB/pixel or more with a fiber length of 10 cm. This image amplifier responds quickly to changes in the image position – with potential for GHz-level frame rates. This unique approach for image amplification offers low noise, high gain, and wide field of view in a compact fiber-based device.

©2007 Optical Society of America

**OCIS codes:** (060.2320) Fiber optics amplifiers and oscillators; (110.2350) Fiber optics imaging.

---

## References and links

1. A. Biswas, M. W. Wright, B. Sani, and N. A. Page, "45 Km horizontal path optical link demonstrations," *Proc. SPIE* **4272**, 60-71 (2001).
2. G. Le Tolguenec, F. Devaux, and E. Lantz, "Imaging through thick biological tissues by parametric image amplification and phase conjugation," *J. Opt.* **28**, 214-217 (1997).
3. B. J. Ainslie, "A review of the fabrication and properties of erbium-doped fibers for optical amplifiers," *J. Lightwave Technol.* **2**, 220-227 (1991).
4. M. J. F. Digonnet, *Rare-Earth-Doped Fiber Lasers and Amplifiers, Second Edition, Revised and Expanded* (Marcel Dekker, 2001).
5. M. Nakamura, K. Kitayama, N. Shamoto, and K. Kaneda, "Two-dimensional erbium-doped image fiber amplifier (EDIFA)," *IEEE J. Sel. Top. Quantum Electron.* **7**, 434-438 (2001).
6. Y. Hu, S. Jiang, T. Luo, K. Seneschal, M. Morrell, F. Smektala, S. Honkanen, J. Lucas, and N. Peyghambarian, "Performance of high-concentration Er<sup>3+</sup>-Yb<sup>3+</sup>-codoped phosphate fiber amplifiers," *IEEE Photon. Technol. Lett.* **13**, 657-659 (2001).
7. S. Jiang, T. Luo, B. Hwang, F. Smektala, K. Seneschal, J. Lucas, N. Peyghambarian, "Er<sup>3+</sup>-doped phosphate glasses for fiber amplifiers with high gain per unit length," *J. Non-Cryst. Solids*, **263&264**, 364-368 (2000).
8. Ch. Spiegelberg, J. Geng, Y. Hu, Y. Kaneda, S. Jiang, and N. Peyghambarian, "Low-noise narrow-linewidth fiber laser at 1550 nm," *J. Lightwave Technol.* **22**, 57-62 (2004).
9. A. Schülzgen, L. Li, V. L. Temyanko, S. Suzuki, J. V. Moloney, and N. Peyghambarian, "Single-frequency fiber oscillator with watt-level output power using photonic crystal phosphate glass fiber," *Opt. Express* **14**, 7087-7092 (2006).
10. A. Chavez-Pirson, B. Hwang, D. Nguyen, T. Luo, and S. Jiang, "Wide field of view image amplifier based on Yb-doped multi-core phosphate optical fiber," in *Proceedings of Conference on Lasers and Electro-Optics, 2005. (CLEO), Vol. 3*, 1978-1980 (2005).
11. A. Chavez-Pirson, W. Tian, D. Nguyen, T. Luo, S. Hocde, Z. Yao, S. Jiang, and N. Peyghambarian, "Multimode-pumped monolithic amplifier arrays based in erbium-doped phosphate glass," in *Optical Society of America's Trends in Optics and Photonics (TOPS) Proceedings, Volume 93 on Optical Amplifiers and their Applications* (2003).
12. A. Chavez-Pirson, B. Hwang, D. Nguyen, T. Luo, and S. Jiang, "New approach to image amplification based on an optically-pumped multi-core optical fiber," *Proc. SPIE* **6289**, 628909 (2006).

## 1. Introduction

Low noise and high speed amplification of weak light images is an important technology focus in a variety of applications, such as air/space surveillance, biomedical imaging, and optical metrology. For example, typical free-space laser communication links suffer from intensity fade-outs due to air turbulence and clouds as frequently as 100 to 1000 times per second [1]. To track the movements of rapidly moving targets in such environments, it is essential to have an image amplifier with a high optical gain and rapid response. In biomedical imaging applications, wavelengths ranging from 600 nm to 1300 nm are commonly used to probe tissues due to their relatively lower absorption [2]. Optical beams at these wavelengths decay in traversing thick tissue primarily due to scattering – resulting in very weak return signals. To overcome the losses, pulsed lasers and sophisticated parametric amplification techniques have been used [2]. To avoid tissue damage, however, lower intensity sources and high gain detectors are strongly preferable.

Conventional approaches to image amplification typically involve image intensifiers using multichannel plates or photocathodes with electron multipliers and fluorescent screens. These methods introduce noise and inevitably discard important information about the light such as its spectral distribution, polarization, and coherence.

Optical fiber amplifiers are capable of boosting optical signals with high gain (>30 dB) and low noise, making optical-electrical-optical conversions unnecessary. Also, they can simultaneously amplify signals at different wavelengths within their gain band. In telecommunication applications, rare earth ion doped optical fiber amplifiers provide a less complicated and cost-effective method of amplification in high data rate networks [3,4]. Although the most common optical fiber amplifier is based on  $\text{Er}^{3+}$  operating at around 1550 nm, other rare earth ions can also provide a wide variety of operating wavelengths from visible, ~480 nm, to infrared wavelengths, ~2  $\mu\text{m}$  [3]. However, these fiber amplifiers amplify light in single mode fibers and are not suitable for amplifying an entire optical image.

Employing the advantages of the optical amplifier, some researchers have studied image amplification with optical fiber technology [5]. They used a multi-core amplifying fiber based silica glass for applications in optical interconnects and signal processing. The amplifying fiber has 3000 cores. Each core diameter is 4.5  $\mu\text{m}$ , and core spacing is 9.0  $\mu\text{m}$ . The 3 meter long amplifier successfully amplified input signals launched to the amplifier. However, in their demonstration using single mode 1.48  $\mu\text{m}$  pump diodes, they achieved a maximum of only <1.2 dB gain per pixel. The pump coupling approach using a single mode pump diode severely limited both the coupled pump power and the achievable gain across the array of pixels.

Recently developed phosphate glass based optical fiber amplifiers and fiber lasers are very attractive devices [6,7]. Phosphate glasses are promising fiber materials because of their higher solubility of rare earth ions compared to conventional silica glass without the major drawbacks associated with elevated doping levels, i.e. concentration quenching or nonlinear up-conversion. For example, typical doping levels for  $\text{Er}^{3+}$  ions can be greater than 5 wt% in phosphate glasses, which is 50 to 100 times higher than is possible with silica glasses [4]. The higher solubility of rare earth ions enables to make compact fiber amplifiers and lasers [8,9]. Importantly, the short length enables high pump absorption per unit length into single mode cores using multimode pump diode sources – which provides a straightforward scaling to higher output power amplification. Also the short fiber length intrinsically prevents introducing undesired nonlinear effects in the amplifiers or lasers.

In this paper we report on an image amplifier based on an  $\text{Yb}^{3+}$ -doped phosphate fiber. The amplifying fiber has 19 cores that are made of heavily  $\text{Yb}^{3+}$ -doped phosphate glasses. The cores act as pixels for image amplification and image guiding. Also a double clad fiber design is applied to confine pump light from high power multimode diode lasers and to efficiently energize the cores uniformly. The amplifier delivered high gain per pixel, ~30 dB with 3 W of

pump power and this was achieved with only 10 cm length of amplifying fiber. Using the image amplifying fiber, we demonstrate image amplification results obtained from stationary and moving input images.

## 2. Optical fiber fabrication

Figure 1 shows a cross-sectional microscope image of the amplifying fiber. It is fabricated by a modified rod-in-tube technique. Three parts of the fiber pre-form – core, inner, and outer cladding, – were fabricated such that they satisfy the required refractive index profile as well as have similar thermal properties necessary for fiber-drawing. These three different phosphate glasses were machined into 1) the core rods, 2) the inner cladding with 19 holes arranged in a hexagonal grid, and 3) the outer cladding. Subsequently these parts were assembled to make a fiber pre-form. Then, the pre-form was drawn into an optical fiber. The core glass is an  $\text{Yb}^{3+}$  6 wt % doped phosphate glass. The nominal core diameter is 5  $\mu\text{m}$ . The nominal core-to-core distance is 14  $\mu\text{m}$  designed so that optical coupling between adjacent cores will not occur. The core elements are formed with a circular cross-section to maintain polarization independent operation. The inner cladding diameter is  $\sim 80 \mu\text{m}$  and outer cladding diameter is  $\sim 140 \mu\text{m}$ . Both the inner and outer cladding glasses are undoped phosphate glasses. The inner cladding confines multimode pump light that is used to energize the cores. Numerical apertures of each core and inner cladding were designed to 0.15 and 0.23, respectively. Thus the full field of view of each core is  $\sim 17.3$  degrees and core filling factor is  $\sim 12\%$ . In this design, each core acts as a pixel and is designed to operate as a single mode waveguide. The gain uniformity across the array generally depends on the core arrangement (i.e. hexagonal or square) inside the inner cladding. This stems from how pump power circulating in the inner cladding is absorbed in the cores. When the number of cores is small ( $< 20$ ), our simulation model shows that the pump power is more efficiently absorbed in cores arranged on a hexagonal grid compared to a square grid. This results in better gain uniformity for a given pump power – and is the reason for our choice of the hexagonal grid in this case. However, when the number of cores is large ( $> 100$ ), the improvement in pump power absorption with core arrangement is not a significant factor anymore. Moreover, no matter the size of the array, increasing the pump power always improves the gain uniformity. In fact, an image amplifying fiber with cores arranged on a  $3 \times 3$  square grid has been demonstrated to result in a highly uniform gain across the array [10,11,12].



Fig. 1. Cross-section of the image amplifying fiber.

## 3. Experiments and discussions

Figure 2 shows the two different experimental arrangements used to characterize the image amplifying fiber; Fig. 2(a) is for the gain experiment of the central pixel, and Fig. 2(b) is for the image amplification experiments. The input signal ( $\sim 7 \mu\text{W}$ ) in Fig. 2(a) was generated

with an  $\text{Yb}^{3+}$ -doped fiber amplified spontaneous emission (ASE) source and a fiber Bragg grating whose center wavelength and spectral bandwidth are 1017 nm and  $<0.15$  nm, respectively, and in Fig. 2(b) the input signal ( $\sim 10$  mW) was generated only with the ASE source. With this type of input source, we had no issue with speckle at the input plane. The pump power was produced by combining 4 fiber pig-tailed 975 nm multimode diode lasers via a fused fiber combiner. The generated signal was coupled into the combiner's signal input port. In this way the combiner provides pump and signal via an output fiber. For the gain experiment, both sides of a 10 cm 19-core amplifying fiber were spliced to passive double clad fibers whose nominal mode field diameter at  $\sim 1550$  nm and inner cladding diameters are  $10.5 \mu\text{m}$  and  $90 \mu\text{m}$ , respectively. The input end of the fiber chain was connected to the combiner's output, and the output end was connected to an optical spectrum analyzer. Figure 3 shows the gain at various pump powers. The gain reaches up to  $\sim 30$  dB at  $\sim 3$  W of total pump power. The gain saturation is not yet observed although the gain curve starts to roll over within the measured pump power range. Beyond 3 W of pump power, the fiber chain started to lase and the gain was clamped. Lasing occurred in this experiment because of small reflections at the splice joints between active and passive fibers. Normal cleaved fiber ends were spliced to form the fiber chain. Since the indices of refraction of the amplifying fiber and the double clad fiber are slightly different, the splice joints feed back some amount of the amplified signal. By implementing angled cleaving and/or index matching that reduce signal feedback, the amplifying fiber's gain will certainly exceed 30 dB.

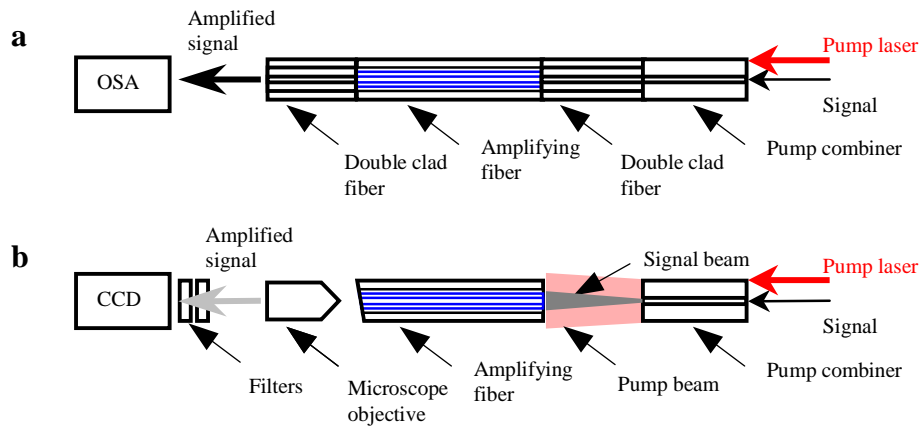


Fig. 2. Schematic of experimental setups. (a) is for gain measurement, and (b) is for imaging experiments.

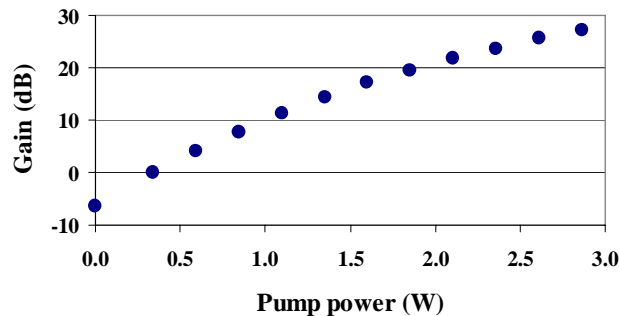


Fig. 3. Gain vs. pump power of a 10-cm long amplifying fiber.

The amplifying fiber's gain uniformity was simulated using NP Photonics' modeling method called the Effective Beam Propagation Method. The results predicted that the gain variation of the fiber would be within 0.5 dB at absolute gain of 30 dB. Figure 4 shows the spatial pattern of ASE from the pixel array of the fiber amplifier measured with 10 cm of the amplifying fiber and  $\sim 2.2$  W of pump power. To obtain this result, the set-up in Fig 2(b) was used except that there was no signal light and the pump combiner's output was closer to the amplifying fiber. As schematically shown in Fig. 2(b), for image amplification experiments the output side of the amplifying fiber was angled cleaved ( $\sim 13^\circ$ ) to prevent lasing. The image in Fig. 4 was recorded with a spectral filter whose transmittance at the pump wavelength was less than 2%. Each core's ASE signal is confined inside the core and the intensities of core ASE signals vary by less than 1 dB. As the simulation predicted, the amplifying fiber's ASE signal distribution is quite uniform. This result implies the cores are uniformly excited by the pump light and will provide uniformly amplified signals.

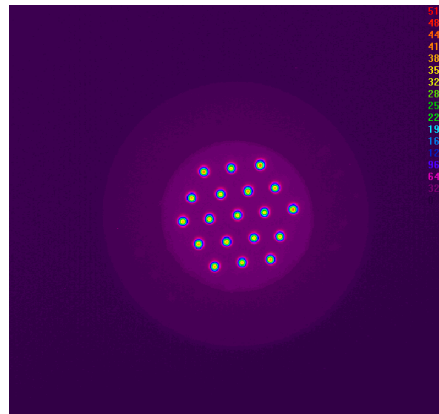


Fig. 4. ASE profile of a 10-cm long amplifying fiber.

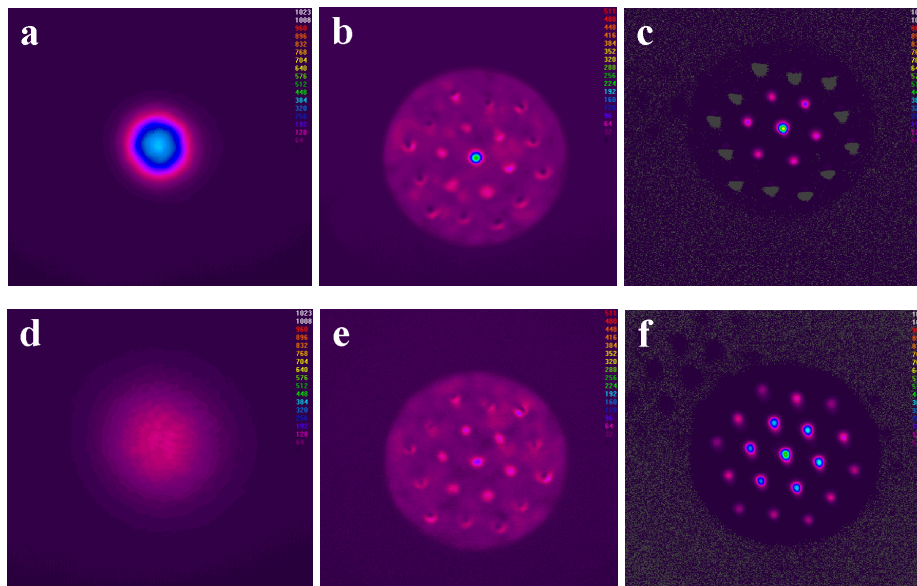


Fig. 5. Image amplification results. (a), (b) and (c) are images of input signal, output without pumping, and amplified signal, respectively. (d), (e) and (f) are those for a spatially broader input pattern.

The stationary image amplification experiment with the amplifying fiber was performed using the setup shown in Fig. 2(b). For the image amplification, input signals with nearly Gaussian profile were generated from the pump combiner's signal output port. Pump sources were again fiber-combined multimode diode lasers, however for imaging, both ends of the amplifying fiber were in air, so pump and signal were free-space coupled. At the output side of the active fiber, amplified images were recorded by a CCD camera with a microscope objective lens. Figure 5 shows the input images, (a) and (d), output images without pumping, (b) and (e), and amplified output images, (c) and (f). Magnifications are the same for all the images in Fig. 5, however the input signal spatial distribution is broader in (d), (e) and (f). The intensity distributions of the amplified images are proportional to the input images' intensity distributions. For example, in Fig. 5(c) the intensity ratio between the pixel at the center and the one next to the center is  $\sim 0.24$ , while the corresponding intensity ratio in the input image, Fig. 5(a), is  $\sim 0.24$ . The images in Fig. 5 were recorded with different ND filter configurations because of higher power in the amplified images and the need to stay within the linear range of the CCD. The net gain in both narrower and broader image inputs in Fig. 5 are  $\sim 20$  dB.

Figure 6 is a movie that demonstrates image amplification of a moving image. For this experiment the setup shown in Fig. 2(b) was used. Compared to the previous image amplification shown in Fig. 5, the difference in this experiment was that the signal was moving during the amplification. The movie shows how this device responds to the spatial and temporal change of the input image signal. At the beginning, the light source is off and after turning it on the image appears slowly due to the light source's warming up. Then the input image starts the movement from the center to right side, and moves to the other side. The response time of the image amplifier is rapid enough that we do not see any image lag or blurring in the CCD read-outs. Although the movie does demonstrate real-time image amplification, the CCD itself and not the image amplifier limits the overall response time.

Rare earth doped optical fiber amplifiers react quickly to changes in signal power – just as in telecommunication applications where data is transmitted at greater than 40 GHz rates. Thus the fiber image amplifier is readily able to respond quickly to changing images without any extra implementation. This quick response is a significant advantage of this fiber amplifier compared to conventional image intensifiers, whose response may be limited by phosphor lifetimes. In contrast, the fast response of the image amplifying fiber potentially offers GHz order frame rates. Of course, in the electronic detection step of an image processing system, the CCD or its equivalent will most likely limit the response time. However, in an all-optical system, or in an all-optical sub-system, there may be no electronic detection. In such a case, the frame rate limit might reside in the image amplifier or in a switching element. It is with this in mind that we mention the potential speed of this image amplifier device – and where it might have a unique benefit. It is an enabling feature for the detection and tracking of fast-moving targets.

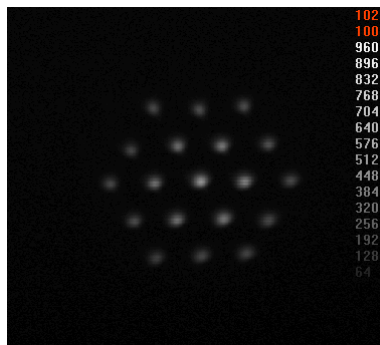


Fig. 6. (154 KB) Movie of an amplified moving image.

Gain measurements show the fiber amplifier's gain can reach ~30 dB or more, under an appropriate pumping and image amplifier interface design. This high gain allows us to detect small signals that are changing rapidly in intensity or sweeping rapidly across the pixel array. Because it is based on fiber amplifier technology, it can also be operated in various modes. In the small signal regime it can act as a linear amplifier with fixed gain. For higher power inputs, it may act as a nonlinear device with a saturated output power. It is an intrinsically low-noise amplifying device with ASE noise contributions that can be minimized – as has been done in telecommunication applications. For a similarly constructed 9-pixel image amplifier a noise figure of less than 6dB was measured [12]. Although the noise figure for this 19-pixel image amplifier was not measured, we anticipate the noise figure to be at this 6 dB level as well. Depending on the wavelength of interest, this general approach to image amplification can be extended to other wavelengths besides the 1000 nm - 1080 nm range of  $\text{Yb}^{3+}$  by using different rare earth doped ions. For example, this same phosphate glass supports high doping of  $\text{Er}^{3+}$  for comparable operation in the 1550nm eye safe range. Extensions are currently underway to increase the number of pixels to above 100 in order to increase the spatial resolution. Although there are technical challenges both from the point of view of fiber fabrication and pumping approaches, we have already made progress in these areas and expect this general approach to have applications in various areas.

#### **4. Conclusion**

We demonstrated image amplification with a 19-pixel optical image amplifier array based on high gain per unit length  $\text{Yb}^{3+}$ -doped phosphate glass optical fiber. Highly  $\text{Yb}^{3+}$ -doped phosphate glass cores provided ~30 dB gain per pixel at a 1017 nm operating wavelength with a 10-cm-long image amplifying fiber. The amplifier provided excellent (<1dB) gain uniformity across the 19-pixel array. The uniformity and linearity of high gain are attractive features for image amplification. It has the interesting feature of responding quickly to changes in image position – with the potential to be compatible with GHz level frame rates such as in all-optical image processing systems. This unique approach makes possible low noise, high gain, and wide field of view image amplification in a compact fiber-based device.

#### **Acknowledgments**

The authors gratefully acknowledge support from the Small Business Innovative Research (SBIR) program of the United States Air Force and the Air Force Research Laboratories under contract number FA9451-05-C-0010.